THE JOURNAL OF PHYSICAL CHEMISTRY LETTERS
A JOURNAL OF THE AMERICAN CHEMICAL SOCIETY

pubs.acs.org/JPCL

Letter

Tuning Selectivity in the Direct Conversion of Methane to Methanol: Bimetallic Synergistic Effects on the Cleavage of C−H and O−H Bonds over NiCu/CeO_2 Catalysts

Pablo G. Lustemberg,* Sanjaya D. Senanayake, José A. Rodriguez, and M. Verónica Ganduglia-Pirovano

Cite This: *J. Phys. Chem. Lett.* 2022, 13, 5589−5596

Read Online

ACCESS | Metrics & More | Article Recommendations | Supporting Information

ABSTRACT: The efficient activation of methane and the simultaneous water dissociation are crucial in many catalytic reactions on oxide-supported transition metal catalysts. On very low-loaded Ni/CeO_2 surfaces, methane easily fully decomposes, $CH_4 \rightarrow C + 4H$, and water dissociates, $H_2O \rightarrow OH + H$. However, in important reactions such as the direct oxidation of methane to methanol (MTM), where complex interplay exists between reactants (CH_4, O_2), it is desirable to avoid the complete dehydrogenation of methane to carbon. Remarkably, the barrier for the activation of C−H bonds in CH_x ($x = 1-3$) species on Ni/CeO_2 surfaces can be manipulated by adding Cu, forming bimetallic NiCu clusters, whereas the ease for cleavage of O−H bonds in water is not affected by ensemble effects, as obtained from density functional theory-based calculations. CH_4 activation occurs only on Ni sites, and H_2O activation occurs on both Ni and Cu sites. The MTM reaction pathway for the example of the Ni_3Cu_1/CeO_2 model catalyst predicts a higher selectivity and a lower activation barrier for methanol production, compared with that for Ni_4/CeO_2. These findings point toward a possible strategy to design active and stable catalysts which can be employed for methane activation and conversions.

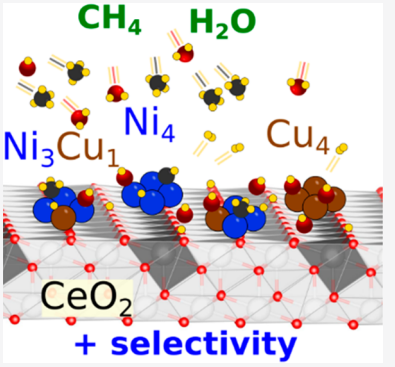

Methane is the main component of natural gas and a major challenge when emitted into the atmosphere because of its contribution to greenhouse effects.[1−3] Its activation is challenging because of the high C−H bond strength,[4−6] but its conversion is of great importance for the synthesis of fuels and chemicals while leading to major environmental benefits.[2,3] Also, water dissociation is an important parallel reaction step in numerous catalytic reactions on oxide-supported transition-metal catalysts, such as the water-gas shift reaction[7−11] and the conversion of methane by steam reforming.[12−14] Moreover, the role of water in the direct catalytic conversion of methane or CO_2 to methanol has recently been highlighted.[15] Therefore, being able to control the ability of catalysts to simultaneously activate methane and dissociate water is highly desirable. However, this is a challenging task, particularly for oxide-supported metal nanoparticles.[16] This is because the activity for C−H and O−H bond breaking can be affected by many factors such as the nature of both the metal and the oxide support, the metal particle size and composition, as well as metal−support interactions.

It has been shown that small Ni nanoparticles on a (111)-oriented ceria model support promote the activation of both O−H and C−H bonds in H_2O and CH_4, respectively, at room temperature, with lower activation barriers than for extended metallic Ni surfaces.[17−21] Studies with other metals such as Pt, Co, and Cu indicated that Pt and Co are also active for C−H bond activation, whereas Cu is not.[18,22]

In the case of low-loaded Ni/CeO_2 catalysts, we have recently shown that the activation of the first C−H bond from CH_4 to yield CH_3 is facile and also that the adsorbed CH_4 undergoes full decomposition to produce C atoms.[12,15,17,20] Both components of the Ni−ceria interface probably participate in the removal of hydrogen from methane to generate carbon. The rapid deactivation through carbon deposition on high-loaded metal-based catalysts is well-known,[17,18,23,24] but this is not the case for low-loaded catalysts. In this regard, for low-loaded Ni/CeO_2 catalysts, no CH_x or C species were observed under methane dry- or steam-reforming conditions ($T > 550$ K).[12,17] In the context of the steam reforming, the OH-mediated carbon removal has been discussed.[12,25] Moreover, in connection with the direct oxidation of methane to methanol (MTM), water was found to play a crucial role in blocking catalytic sites where methyl species could fully decompose, an essential factor for diminishing the production of CO and CO_2, and in generating

Received: March 27, 2022
Accepted: June 8, 2022
Published: June 14, 2022

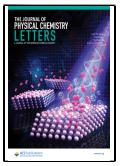

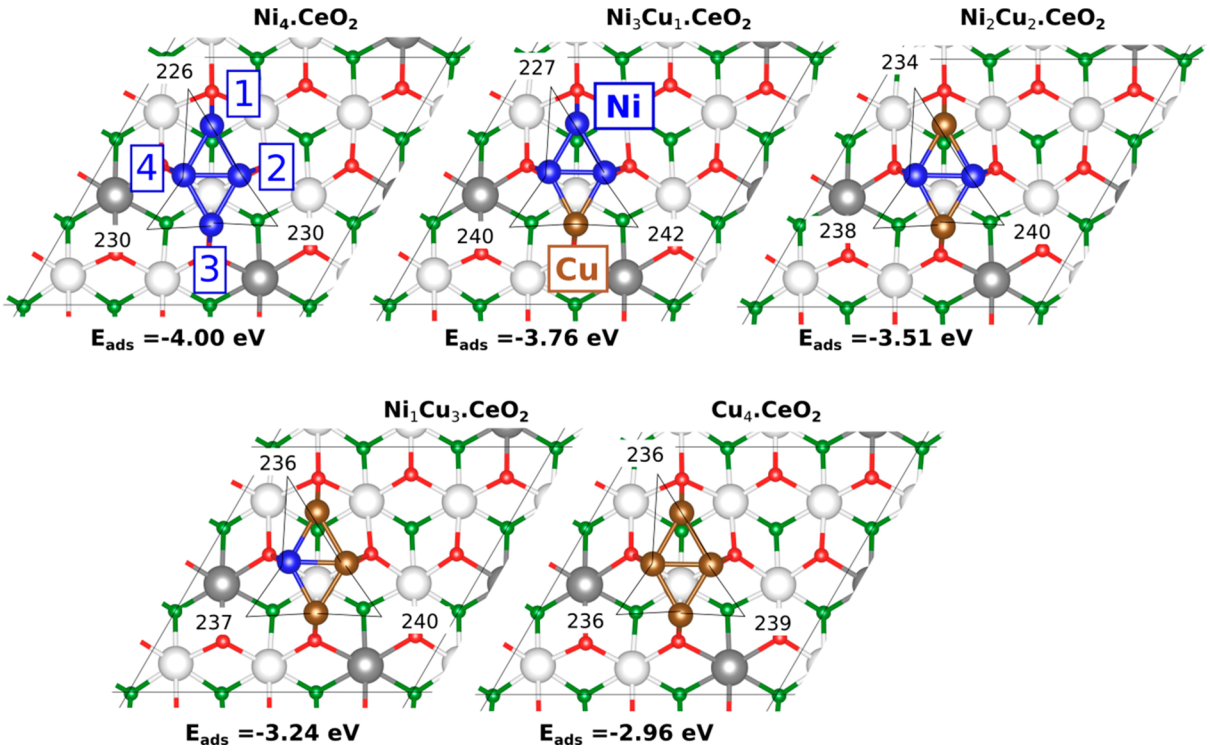

Figure 1. Adsorbed $Ni_{4-x}Cu_x$ (x = 0 to 4) clusters on $CeO_2(111)$. Ni and Cu atoms are depicted in blue and brown, respectively, while surface/subsurface oxygen atoms are in red/green, Ce^{4+} in white, and Ce^{3+} in gray. Selected interatomic distances (in pm) are indicated. The average adsorption energy for each model is indicated (with respect to the isolated Cu_{gas} and Ni_{gas} atoms, in eV). The four metal atoms are labeled according to their positions with respect to the ceria surface as 1 to 4.

sites on which methoxy CH_3O species and ultimately methanol can form and desorb.[15] However, is there another strategy to achieve a similar control of the reaction selectivity by minimizing the decomposition of CH_x and CH_3O intermediates?

In the field of heterogeneous catalysis by metals, bimetallic catalysts are promising for performing challenging chemical transformations,[26−31] and the ensemble effect is a well-known phenomenon.[32] The main feature of this effect is that reactions are sensitive to alloying with a second metal within the group of adjacent atoms of the active metal that are required for forming chemisorption complexes. The effects of alloying may be rationalized by a combination of geometric and electronic effects, the separation of which is not always straightforward. The concept of geometric ensemble implies that the metal atoms in the surface of the alloy keep their individuality and are only influenced by their immediate environment. Electronic effects in alloy catalysts refer to the formation of a bond between two different metals that can induce substantial electronic perturbations leading to changes in the chemical and catalytic properties of the bonded metals.[26−31] In this context, it is important to establish if bimetallic nickel catalysts, such as $NiCu/CeO_2$, can be useful for tuning the degree of dehydrogenation of CH_x (x = 1−3) species on Ni/CeO_2 surfaces, which is critical for preventing coke formation and crucial in the direct partial oxidation of methane to methanol or in the conversion of CH_x groups into high-value chemicals like olefins or aromatics.

In this work, we use density functional theory-based calculations within the DFT+U approach, including long-range dispersion corrections, to study in detail the binding and dehydrogenation of methane, as well as the dissociation of water on $Ni_{4-x}Cu_x/CeO_2(111)$ bimetallic surfaces with five different concentration ratios of 0%, 25%, 50%, 75%, and 100% (hereinafter referred to as $Ni_{4-x}Cu_x.CeO_2$). In addition, the complete reaction pathway for the direct oxidation of methane to methanol was calculated for the example of $Ni_3Cu_1/CeO_2(111)$ and compared to that for $Ni_4/CeO_2(111)$. Our results reveal that by adding Cu to low-loaded Ni/CeO_2 catalysts, the activation energy barrier for the cleavage of C−H bonds in methyl CH_3 species significantly increases and that a small percentage of Cu is already sufficient for the effect to be noticeable, whereas it does not appreciably affect the ability of the system to active O−H bonds in water. The results further suggest that, on NiCu bimetallic catalysts, the formation of methoxy species from methyl and oxygen species is favored over further dehydrogenation of the methyl species and that the activation energy for the formation of methanol from methoxy and H species is smaller compared with monometallic Ni catalysts.

The models used are derived from the stable planar rhombohedral Ni_4 cluster on $CeO_2(111)$[20,33,34] by replacing one, two, and up to the four Ni atoms by Cu, as reported by Salcedo et al.[35] (see Figure 1; for details on the models, stability, and computational methods, see the Supporting Information). These $Ni_{4-x}Cu_x$ clusters are compact but allow a study of the electronic and ensemble effects present in $NiCu/CeO_2$ bimetallic systems.[35] Moreover, the planar $Ni_4.CeO_2$ model mimics the essential features of the experimental Ni/CeO_2 catalysts for the direct conversion of methane to methanol ($Ni^{\delta+}/CeO_2$),[15] and in previous works,[17,22,36] we have investigated such ceria-supported small metallic (Ni, Co, Pt) clusters as theoretical model catalysts in close collaboration with studies employing experimental model catalysts, as well as

https://doi.org/10.1021/acs.jpclett.2c00885
J. Phys. Chem. Lett. 2022, 13, 5589−5596

real (powder) systems for reactions such as the dry-reforming of methane.

The $Ni_{4-x}Cu_x.CeO_2$ systems involve Ni and Cu species with similar electron donor−electron acceptor properties, and the flow of charge is here influenced by the existence of the Ni−Cu bond in the bimetallic clusters, the geometrical arrangement of the atoms, and the existence of the ceria support. As a result of strong metal−support interactions, all clusters reduce the ceria support with the formation of two Ce^{3+} (Figure 1). The calculated Bader charges indicate that all atoms in the ceria-supported $Ni_{4-x}Cu_x$ (x = 0 to 4) clusters lose charge (i.e., $Ni_{4-x}^{\delta+}Cu_x^{\delta+}.CeO_2$, Table S1). However, the atoms that lie along the longer diagonal (atoms 1 and 3, Figure 1), coordinated to two other metal atoms, transfer more charge than those that lie along the shorter diagonal (atoms 2 and 4), which are surrounded by three metal atoms. This is in line with the flow of charge observed for the gas-phase clusters, which result from the removal of the $CeO_2(111)$ support from the $Ni_{4-x}Cu_x.CeO_2$ systems, without further optimization of the geometry (hereinafter referred to as $Ni_{4-x}Cu_x$.gas, Table S1), according to which, the atoms 2 and 4 in 3-fold coordination, give charge to the atoms 1 and 3 in 2-fold coordination. Therefore, it could be summarized by saying that the atoms with the most charge in the gas phase are the ones that transfer the most charge to the ceria support. Furthermore, we also examined the effect of forming bimetallic clusters on the d-projected density of states of the metal atoms for the supported and gas-phase clusters (Table S2). As expected, an increase in the percentage of occupied Ni d-states in the $Ni_{4-x}Cu_x.CeO_2$ and $Ni_{4-x}Cu_x$.gas systems (x = 1−3), compared with $Ni_4.CeO_2$ and Ni_4.gas, respectively, is observed. In the case of the occupied Cu d-states, the effect is the reverse with an upward shift of the center of the atom-project d-band relative to the Fermi level.

The most stable configurations of the $CeO_2(111)$-supported $Ni_{4-x}Cu_x$ (x = 0 to 4) clusters (Figures 1 and S1) were used to study the activation of both CH_4 and H_2O.

In the following, we will discuss the first hydrogen abstraction from CH_4, i.e., $CH_4 \rightarrow CH_3$+H, first for the monometallic $Ni_4.CeO_2$ and $Cu_4.CeO_2$ surfaces, as compared with Ni and Cu(111), respectively. The dissociation of CH_4 is slightly exothermic with ΔE= −0.09 eV over the extended Ni(111) surface, whereas over Cu(111) is endothermic with ΔE= +0.64 eV (Table S3, Figures S2 and S3). Moreover, the first C−H bond cleavage over these surfaces is very difficult at low temperatures, because of large energy barriers of 0.90 and 1.42 eV for the Ni and Cu surfaces, respectively (Figures 2b and S2).[18,22] This is in clear contrast with the results obtained for small monometallic Ni_4 and Cu_4 particles supported on $CeO_2(111)$, for which the reaction is highly exothermic with ΔE = −0.8 and −1.05 eV (Figure 2a, Table S3), respectively. In addition, the reduction of the energy barriers, compared to the corresponding extended (111) metal surfaces, is noticeably, particularly for the case of the Ni_4 particles (Figure 2a). The barrier over $Ni_4.CeO_2$ is 0.14 eV, whereas that over $Cu_4.CeO_2$ is 1.08 eV. This is in line with the results of experiments that show that methane dissociates on low-loaded Ni/CeO_2 at temperatures as low as 300 K, generating CH_x and CO_x species on the catalyst surface, whereas Cu/CeO_2 has a negligible activity.[18]

In Figure 2a, the dissociation products correspond to stable chemisorbed states geometrically close to the corresponding transition state structures, with both CH_3 and H species on the metal clusters. We observe that paths that involve simultaneous interactions of methane with the Ni or Cu sites and oxygen centers of the ceria support (Figure S4), with CH_3 species adsorbed on the metal clusters and H forming OH species in the final states, did not lead to lower activation barriers when compared with the cases in which both CH_3 and H species bind to the chemically modified supported cluster. This is similar to the case of Pt_4 clusters on $CeO_2(111)$.[22]

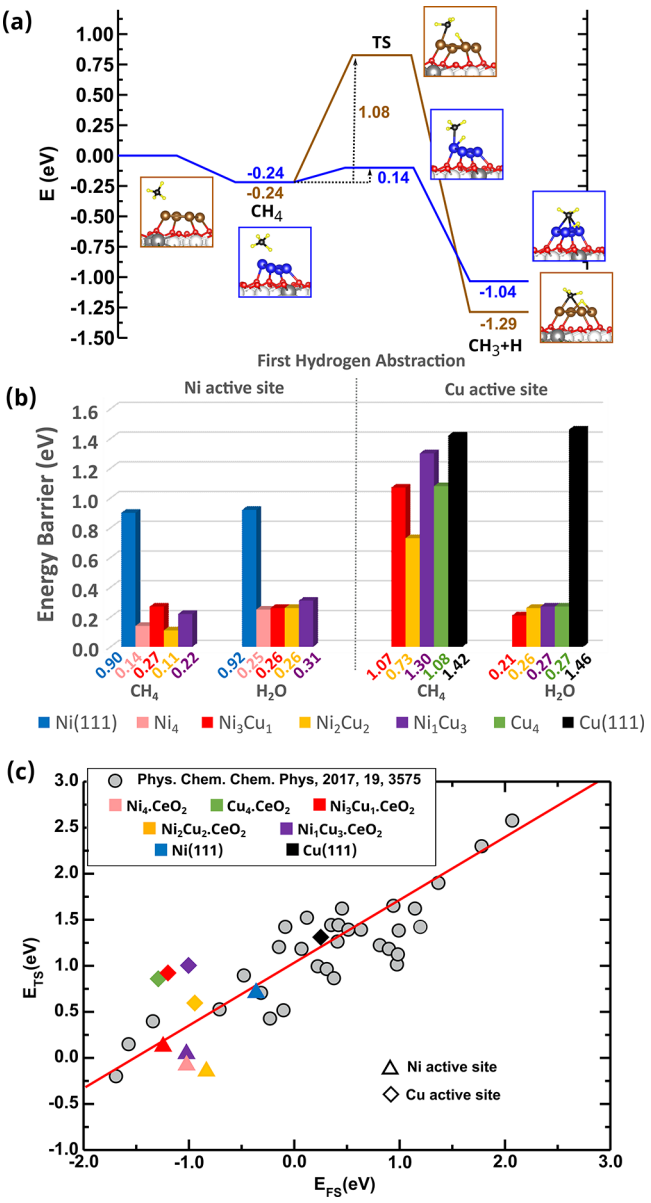

Figure 2. (a) Energy profile for the $CH_4 \rightarrow CH_3$+H reaction on $Ni_{4-x}Cu_x$ (x = 0 to 4) clusters on $CeO_2(111)$. The structures shown on the left and right of the reaction pathways correspond to the side views of the optimized initial (molecularly adsorbed) and final (dissociated) states used in the search of the transition state structure (TS). (b) Lowest activation energy barriers for the $CH_4 \rightarrow CH_3$+H and $H_2O \rightarrow$ OH+H reactions channels offered by Ni and Cu sites in the $Ni_{4-x}Cu_x$ clusters (x = 0 to 4) on $CeO_2(111)$ and for the extended Ni and Cu(111) surfaces. (c) Scaling relation for the surface-stabilized pathway ($E_{TS} = 0.67E_{FS} + 1.04$, red line), according to ref 37. Shown are the E_{TS} and E_{FS} values for the paths with lowest activation barriers among those over Ni and Cu sites in the $Ni_{4-x}Cu_x$ clusters (x = 0 to 4) on $CeO_2(111)$ and for the extended Ni(111) and Cu(111) surfaces (not included in the linear fit).

https://doi.org/10.1021/acs.jpclett.2c00885
J. Phys. Chem. Lett. 2022, 13, 5589−5596

The factors leading to the better ability of the Ni/CeO_2 system to cleave the first C−H bond, as compared with Cu/CeO_2, are related to the distinct adsorption properties of the former. The careful inspection of the adsorption of the CH_4 molecule on these systems reveals that on $Ni_4.CeO_2$, the molecule comes closer to the surface than on $Cu_4.CeO_2$, cf. the C−Ni distance of 212 pm and C−Cu of 261 pm (Table S4, Figures S5a and S6a). The closer approach can be correlated with the clear difference between the d and d_{z^2} projected density of states on the Ni and Cu atom over which CH_4 dissociates, with approximately 67% and 99% occupation of the d_{z^2} states, respectively (Figure S7, Table S2). Therefore, the Pauli repulsion to the methane's frontier orbital is reduced in the case of the $Ni_4.CeO_2$ surface. Furthermore, the comparison with the corresponding d_{z^2} occupancy of approximately 84% and 100% in the free-standing Ni_4.gas and Cu_4.gas clusters, respectively (Table S2), reveals that in the case of Ni_4, the d_{z^2} states become less occupied upon adsorption of the metal cluster onto the ceria surface, resulting in the partial depopulation of the d_{z^2} states (from 84% to 67%) that facilitates the approach of the CH_4 molecule and the easier cleavage of the first C−H bond. Such ligand effect is a consequence of the bonding of the metal atoms of the cluster to the surface oxygen atoms of the ceria support, which is much more pronounced in the case of small supported Ni clusters.

In both $Ni_4.CeO_2$ and $Cu_4.CeO_2$ systems, charge is transferred to the CH_4 molecule upon adsorption, which is significantly larger for $Ni_4.CeO_2$ than for $Cu_4.CeO_2$, as reflected by the corresponding increase in the Bader charge of the C atom, namely, 0.16 $|e^-|$ and 0.06 $|e^-|$ for $Ni_4.CeO_2$ and $Cu_4.CeO_2$, respectively, with respect to the gas-phase molecule (Table S3). Most importantly, the C−H bond that will ultimately be cleaved is more elongated for $Ni_4.CeO_2$ than for $Cu_4.CeO_2$ (cf. 119 and 111 pm, respectively, Table S3, Figures S5a and S6a, with 110 pm in the gas-phase), facilitating bond breaking.

We will now address the effect of alloying Ni with Cu on the activation barrier for the CH_4 to CH_3+H reaction. For extended Cu-doped Ni surfaces, it has been found that barriers over Ni sites are larger for the Cu-doped surfaces than for the corresponding undoped ones.[38,39] For example, for the case of the Ni(111) with a surface Cu dopant concentration of 1/4, the barrier is 1.3 times higher.[38] The CH_4 to CH_3+H reaction channels with the lowest activation energy barriers offered by the Ni and the Cu sites of the CeO_2(111)-supported bimetallic $Ni_{4-x}Cu_x$ clusters (x = 1 to 3) are exothermic with ΔE values within the −0.5 to −1.1 eV energy range (Table S3). Figure 2b compares the corresponding activation energy barriers (cf. Figure S4). It is evident that barriers are smaller for Ni sites, lying within the 0.1−0.3 eV energy interval, whereas those over Cu sites lie within a 0.7−1.3 eV interval. As in the case of the extended Cu-doped Ni surfaces reported in the literature,[38] the lower energy barrier over Ni sites on the bimetallic $Ni_{4-x}Cu_x.CeO_2$ surfaces could be up to a factor of 2 higher than over the corresponding Ni site on the monometallic $Ni_4.CeO_2$ surface due to the presence of the neighboring Cu atoms, although barriers are never higher than 0.3 eV (cf. for example 0.14 and 0.27 eV for $Ni_4.CeO_2$ and $Ni_3Cu_1.CeO_2$, respectively, Figures 2b and S4). These changes can be attributed to the interacting electronic effects of Ni and Cu atoms. For example, comparing the Ni-projected density of states for the d-orbitals of the Ni atom over which CH_4 dissociates over the $Ni_4.CeO_2$ and $Ni_3Cu_1.CeO_2$ surfaces (cf. atom number 4 in Figure S7, Table S2), we observe that adding Cu results in the lowering of the Ni d-band center and the partial population of the d_{z^2} orbitals (from 67% to 79%), which leads to a decrease in molecule−surface interaction for $Ni_3Cu_1.CeO_2$, as reflected by a CH_4 molecule positioned further away from the surface (from 212 for $Ni_4.CeO_2$ to 270 pm $Ni_3Cu_1.CeO_2$, Table S4, Figures S5a and S8a), and a less charge transferred to the alkane molecule upon adsorption (from 0.16$|e^-|$ for $Ni_4.CeO_2$ to 0.08$|e^-|$ for $Ni_3Cu_1.CeO_2$, Table S4). Furthermore, since Ni sites proved to be highly reactive for abstracting H from chemisorbed CH_4 molecules, the reactivity differences have been correlated to the binding of the H atom to the supported clusters (with respect to 1/2 H_2), calculated by removing the CH_3 species from the TS structures, without further optimization (Table S5, Figure S16).

In the case of the Cu sites on the $Ni_{4-x}Cu_x.CeO_2$ surfaces, energy barriers are higher than 0.7 eV, and somewhat more pronounced variations are observed with the composition of the cluster than those found for Ni sites (Figure 2b), with the lowest barrier of 0.73 eV for the Ni_2Cu_2 cluster. Inspection of the Cu-projected densities of states (Figure S7, Table S4) does not reflect noticeable differences in the population of the d_{z^2} orbitals (∼99%) of Cu sites in the $Ni_{4-x}Cu_x.CeO_2$ (x = 1−4) surfaces. However, differences in the activation barriers on Cu sites correlate with the binding of the H atom to the supported clusters (with respect to 1/2 H_2), calculated by removing the CH_3 species from the TS structures, without further optimization, according to which the stronger the H binding, the more stabilized the TS structure will be, and the smaller the barrier. The binding of the H atom on the Ni_2Cu_2 cluster is approximately 0.2 eV stronger, as compared with Ni_3Cu_1 and Ni_1Cu_3 (Table S5, Figure S17). Furthermore, inspection of the transition state structures for activation on Cu sites (Table S6, Figures S6b, S8h, S9e, S10e) reveals geometrical differences, particularly with regard to the H atom in the generally elongated C−H bond. The higher stabilization of the TS structure for the CH_4 to CH_3+H reaction over Cu sites in the Ni_2Cu_2 cluster can be related to the fact the H atom is close to two Ni atoms, with Ni−H distances of 187 and 194 pm (Table S6), compared with one Ni atom in the Ni_3Cu_1 and Ni_1Cu_3 clusters, with Ni−H distances of 190 and 213 pm, respectively. We further note that the adsorption energy of a H atom after geometry optimization on the supported clusters follows the the order of Ni_4 > Ni_2Cu_2 > Ni_3Cu_1 ∼ Ni_1Cu_3 > Cu_4 (Figure S17).

Summarizing, as stated above, the presence of Ni sites in bimetallic $Ni_{4-x}Cu_x$ clusters on CeO_2(111) will always be the reason why these clusters will be highly active for the CH_4 to CH_3+H reaction because the energy barriers are less than 0.3 eV. The activity of Ni and inactivity of Cu in the bimetallic $Ni_{4-x}Cu_x$ clusters is controlled by ligand effects, which are much more pronounced in the case of Ni sites than on Cu ones.

As previously discussed for the case of the ceria-supported monometallic Ni_4 cluster,[22] strong interactions between ceria and the small clusters lead to the stabilization of the CH_3+H products, as well as the CH_4 molecule in ways that the cleavage of the first C−H bond is significantly easier than predicted by a simple scaling relation[37] between the calculated energies of the transition state structures for methane activation, E_{TS} (referenced to gas-phase CH_4 and the clean surface) and the

https://doi.org/10.1021/acs.jpclett.2c00885
J. Phys. Chem. Lett. 2022, 13, 5589−5596

energy of the CH_3+H final state, E_{FS}. Similarly, for the reaction channels offered by Ni sites in the $Ni_{4-x}Cu_x$ clusters (x = 0 to 3) on CeO_2, substantial deviations of up to 0.7 eV from predicted E_{TS} values are observed (Figure 2c, Table S3), implying calculated activation barriers up to 0.7 eV lower than predicted. However, the contrary is observed for the Cu sites (Figure 2c, Table S3), with E_{TS} values that are up to 0.7 eV higher than the ones predicted by the linear scaling relation. Despite the relatively high stability of the final state of the reaction channels offered by the Cu sites, the nearly fully populated Cu d and d_{z^2} states (Table S2) do not allow initial adsorption states that facilitate the breaking of the C−H bond, and consequently, the activation barriers are high (Figure 2d). These results illustrate that the *nature* of the metal site in low-loaded bimetallic-oxide systems and strong metal−support interactions are crucial to obtaining an improved activity toward the first C−H bond activation. However, what happens in the case of the decomposition of the methyl CH_3 species when alloying Ni with Cu?

As mentioned above, in the case of low-loaded monometallic Ni/CeO_2 catalysts, not only the cleavage of the first C−H bond from CH_4 is easy but also the full decomposition of the formed CH_3 species.[12,15,17,20] The calculated reaction profile for the dissociation from CH_4 up to CH over the $Ni_4.CeO_2$ model catalyst is shown in Figure 3. The first H abstraction

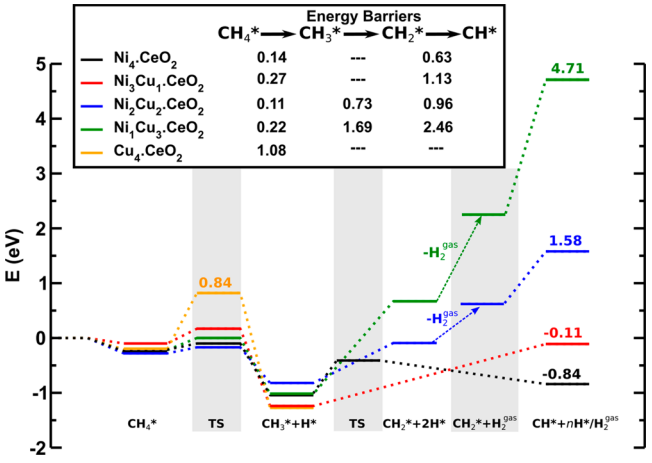

Figure 3. Energy profile for the CH_4 decomposition to CH on $Ni_{4-x}Cu_x$ (x = 0 to 4) clusters on CeO_2(111). Energies of all states are referred to those of the clean surface and gas-phase CH_4. The stars indicate chemisorbed species, and the arrows represent the removal of chemisorbed hydrogen as gas-phase H_2.

produces CH_3 and H species bound to the Ni cluster with a very low activation barrier of 0.14 eV, as discussed above. The subsequent dissociation of the adsorbed CH_3 produces directly CH and 2H species, also bound to the Ni cluster, with a barrier of 0.63 eV. The reaction $CH_4 \rightarrow CH_3$+H $\rightarrow$ CH + 3H is exothermic with ΔE= −0.6 eV, and the highest barrier of 0.63 eV can be overcome under typical experimental conditions for the dry or steam reforming of methane,[12,17] as well as those for its conversion to methanol.[15] Further dissociation of the CH species produces C adatoms.[12,17] In the case of the direct oxidation of methane to methanol, making the full decomposition of CH_3 species energetically unfavorable is crucial for improving reaction selectivity, that is, hindering the path that would lead to CO/CO_2 formation.

The dramatic synergistic effect of ceria-supported bimetallic $Ni_{4-x}Cu_x$ clusters (x = 1 to 3) on the decomposition of methyl species is shown in Figure 3. As discussed above, the first H abstraction will always occur over Ni sites. However, the combination of Ni with a small amount of Cu, forming the $Ni_3Cu_1.CeO_2$ surface, induces important changes in the energy profile from CH_4 to CH, as compared with that for the monometallic $Ni_4.CeO_2$ system. The $CH_4 \rightarrow CH_3$+H $\rightarrow$ CH + 3H reaction over the bimetallic $Ni_3Cu_1.CeO_2$ surface is slightly exothermic with a minimal energy gain (thermoneutral). The lowest activation barrier for the cleavage of the first C−H bond from CH_4 over Ni sites amounts to 0.27 eV as discussed above (Figure 2b), but the following dissociation of CH_3+H that produces CH+3H species, has a barrier of at least 1.13 eV (Figure 3). The potential energy surface goes uphill and no transition state structure has been found. The barrier for the decomposition of the CH_3 species over the bimetallic $Ni_3Cu_1.CeO_2$ surface is approximately 1.8 times higher than that for the monometallic $Ni_4.CeO_2$ surface with a barrier of 0.63 eV, as discussed above.

The higher activation barrier for the CH_3+H $\rightarrow$ CH + 3H reaction over the bimetallic $Ni_3Cu_1.CeO_2$ surface, compared with $Ni_4.CeO_2$, can be related to the significantly lower stability of the CH + 3H final state in $Ni_3Cu_1.CeO_2$ (cf. − 0.11 and −0.84 eV for $Ni_3Cu_1.CeO_2$ and $Ni_4.Cu_1.CeO_2$, respectively). We observe that the final state is to a great extent stabilized by the binding of the H species. The binding of the 3H atoms to the supported clusters (with respect to 1/2 H_2), calculated by removing the CH species from the final state structures, without further relaxation, is −0.13 and −1.15 eV for $Ni_3Cu_1.CeO_2$ and $Ni_4.CeO_2$, respectively. On the $Ni_3Cu_1.CeO_2$ surface, two H atoms bind to one Ni atom (Ni−H: 146 and 157 pm) and the other H forms a bridge between Ni and Cu atoms (Ni−H: 176 pm and Cu−H: 166 pm), whereas on $Ni_4.CeO_2$, two H atoms bind in bridge position between two Ni atoms (2× Ni−H: 159 and 160 pm) and the other binds to a single Ni atom (Ni−H: 157) (Figure S18).

Finally, we briefly mention the effect of adding more Cu (50 to 75%) to the bimetallic $Ni_{1-x}Cu_x.CeO_2$ model catalyst on the decomposition of methyl species. In contrast to the $Ni_4.CeO_2$ and $Ni_3Cu_1.CeO_2$ surfaces for which CH+2H species are produced, over the $Ni_2Cu_2.CeO_2$ and $Ni_1Cu_3.CeO_2$ surfaces, the dissociation of CH_3 species initially produces CH_2+H (Figure 3). In both cases, the reaction is highly endothermic with barriers of at least 0.73 and 1.69 eV for the $Ni_2Cu_2.CeO_2$ and $Ni_1Cu_3.CeO_2$ surfaces, respectively. Accordingly, as for the bimetallic $Ni_3Cu_1.CeO_2$ system discussed above with a very low proportion of Cu, the decomposition of CH_3 species would also be suppressed if the proportion of Cu further increases.

The above results suggest that the full decomposition of CH_3 species to C observed for low-loaded Ni/CeO_2 systems,[12,15,17,20] could already be avoided by mixing small amounts of Cu with Ni. This implies that the selectivity of the conversion of CH_x groups into high value chemicals such as methanol or other hydrocarbon species can be controlled by the so-called geometric ensemble effects in catalysis.[40,41] In practical terms, by adding small amounts of an inactive metal such as Cu to form a bimetallic $Ni_{1-x}Cu_x/CeO_2$ catalyst, the large ensembles of Ni sites that lead to full decomposition of CH_3 and deactivation by carbon deposition would not exist, which corresponds to a geometric or structural effect.

https://doi.org/10.1021/acs.jpclett.2c00885
J. Phys. Chem. Lett. 2022, 13, 5589−5596

In brief, for low-loaded Ni/CeO_2 catalysts, it is the high reactivity of chemisorbed CH_4 toward decomposition over small Ni particles, chemically modified by the presence of the reducible ceria support, that activates the formation of CH_3 species and the subsequent dehydrogenation reactions. The full CH_4 decomposition reaction pathway can be modified by employing ceria-supported bimetallic $Ni_{1-x}Cu_x$ particles. Through tuning the Ni/Cu atomic ratios in the bimetallic Ni_xCu_y particles, the extent of the Ni ensembles can be controlled, separating them by inert Cu for C−H bond cleavage, which leads to the suppression of the dehydrogenation of the CH_3 species. To verify this hypothesis, we have calculated the complete reaction pathway for the direct oxidation of methane to methanol with oxygen: $CH_4 + O \rightarrow CH_3 + H + O \rightarrow CH_3O + H \rightarrow CH_3OH$ for the example of $Ni_3Cu_1.CeO_2$, compared with $Ni_4.CeO_2$. In line with our previous work,[15] an O atom is preadsorbed on both metallic clusters (differences between the values reported in this and previous work for $Ni_4.CeO_2$,[15] are related to the inclusion vdW interactions in this work). The results indicate that the first hydrogen abstraction from CH_4, in the presence of O species, has relatively low barriers, between 0.4 and 0.6 eV for both surfaces (Figure 4). The cleavage of a C−H bond from the CH_3 species is more likely to occur on $Ni_4.CeO_2$, since it has an activation barrier which is by 0.38 eV lower than that for formation of methoxy species (Figure 4). However, on $Ni_3Cu_1.CeO_2$, the formation of methoxy species becomes probable since the activation energy for the formation of CH_3O species is comparable—or even lower—than that for the further dehydrogenation of CH_3 species (Figure 4). We further calculated the formation of CH_3OH from CH_3O+H species and found that it is favored over the $Ni_3Cu_1.CeO_2$ surface compared with $Ni_4.CeO_2$, since the activation barrier is by 0.23 eV lower for the supported Ni_3Cu_1 cluster. Hence, the addition of Cu to ceria-supported Ni particles could increase the selectivity toward methanol formation from CH_4 and O_2.

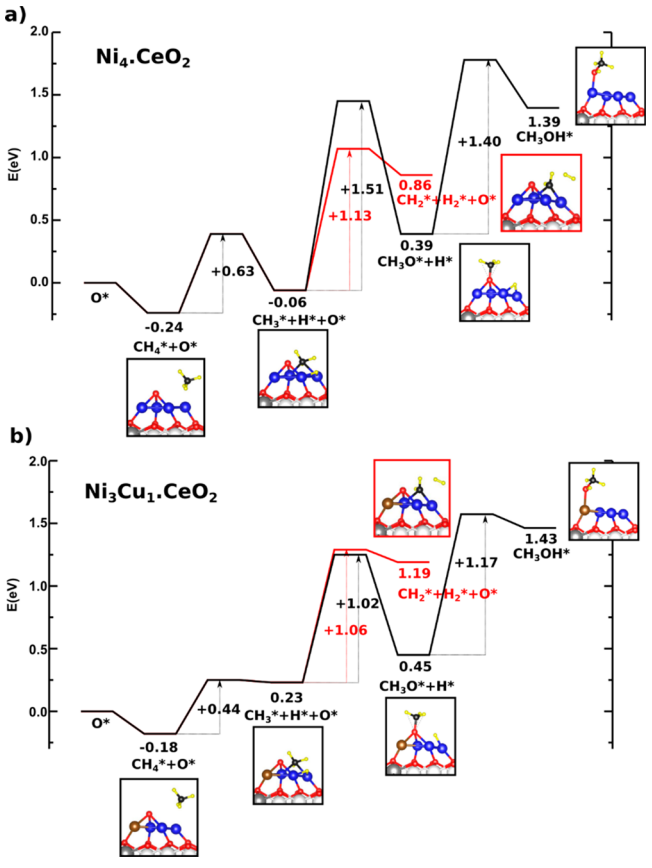

Figure 4. Full reaction mechanism for the direct conversion of methane to methanol from chemisorbed CH_4 and O species over (a) $Ni_4.CeO_2$ and (b) $Ni_3Cu_1.CeO_2$ surfaces.

In the following, we briefly address the role of active site isolation in the reactivity of $Ni_{1-x}Cu_x/CeO_2$ systems for O−H bond cleavage from water, because water was found to enable the catalytic conversion of CH_4 to methanol over monometallic Ni/CeO_2 surfaces by site-blocking.[15]

The dissociation of H_2O on the extended Ni(111) and Cu(111) surfaces at low temperatures is very difficult because of large energy barriers of 0.92 and 1.46 eV, respectively (cf. Figures 2b and S2), in line with previous results.[19,42] Earlier experimental and theoretical studies have shown that on low-loaded Ni/CeO_2 systems,[12,15,19] water binds strongly and would easily dissociate at interfacial Ni sites ($Ni^{\delta+}$) in direct contact with the CeO_2 support, where Ni and O sites can work cooperatively, that is, in the final state, OH species are bound to the Ni nanoparticle, whereas H species form OH species with surface oxygen atoms. Over the $Ni_4.CeO_2$ model catalyst, the barrier for such a cooperative reaction pathway is 0.25 eV (Figure 2b and S4), whereas those for noncooperative pathways over $Ni^{\delta+}$ sites are within the 0.4−0.5 eV range (Figures S4). Similarly, on all of the $Ni_{4-x}Cu_x.CeO_2$ surfaces (x = 1 to 3), the strong binding of water molecules on Ni sites (Figures S19−S22) and their easy dissociation are predicted, with activation barriers within the 0.2−0.3 eV range for cooperative pathways (Figures 2b and S4) and the 0.3−0.7 eV range for noncooperative ones (Figure S4).

As for the interfacial Cu sites ($Cu^{\delta+}$), contrary to the extended metallic Cu(111) surface that does not show reactivity toward H_2O dissociation, but similarly to Ni sites ($Ni^{\delta+}$) in the $Ni_{4-x}Cu_x.CeO_2$ systems, water binds strongly and would dissociate with or without participation of the ceria support with barriers that are below 0.3 eV (Figures 2b and S4). Therefore, it can be concluded that Ni sites in low-loaded bimetallic $Ni_{4-x}Cu_x$ clusters (x = 0 to 3) on $CeO_2(111)$ will bind and easily activate both CH_4 and H_2O, whereas Cu sites will be active toward H_2O dissociation but *not* CH_4. The reason for the distinct behavior of the Cu sites can be related to the higher initial stabilization of molecular water as compared to methane on such sites. For example, the initial adsorption energy of CH_4 and H_2O molecules on the monometallic $Cu_4.CeO_2$ surface is −0.24 and −0.81 eV, respectively (Figures S12 and S23, Tables S4 and S8), with Cu−C and Cu−O bond distances of 261 and 194 pm, respectively. Moreover, the O−H bond in the molecularly adsorbed water that will eventually break is somewhat more elongated than the other (cf. 101 and 98 pm, Table S8), while the corresponding difference between the C−H bonds is smaller (cf. 111 and 110 pm, Table S4).

In summary, this work has addressed the difficult problem of designing a catalyst that would allow the control of the degree of dehydrogenation of CH_3 species that form after the cleavage of the first C−H bond in CH_4 and at the same time is active for the possibly simultaneous dissociation of H_2O. NiCu bimetallic clusters supported on the $CeO_2(111)$ surface with different Ni/Cu ratios were investigated as model catalysts for the activation of C−H and O−H bonds. On the basis of the

https://doi.org/10.1021/acs.jpclett.2c00885
J. Phys. Chem. Lett. 2022, 13, 5589−5596

results obtained in this work, as well as on the previous knowledge on systems consisting of monometallic Ni clusters supported on ceria, it can be concluded that the presence of Ni sites in the NiCu bimetallic clusters is essential for C−H bond breaking in CH_4, where strong interactions between the small metal clusters in direct contact the with the ceria support lead to the stabilization of both the CH_4 molecule and the CH_3+H dissociation product, producing active and stable catalysts for methane activation under very mild conditions. Moreover, CH_3 species fully decompose on Ni ensembles. A design strategy is here suggested to tune the degree of dehydrogenation of CH_3 species that consists of mixing Ni with Cu such that the surface Ni ensembles in the NiCu bimetallic particles only allow for the cleavage of the desired number of C−H bonds in CH_3. By using such catalysts, the high reactivity toward breaking the first C−H bond in the alkane will not be affected, but the outcome of its conversion will, because CH_3 species will not decompose on Cu. The results also show that the strategy does not affect the ability of Ni/CeO_2 catalyst for O−H bond cleavage. The findings underscore the idea that by tuning the composition of supported bimetallic nanoparticles as well as manipulating metal−support interactions, various selectivities can be obtained.

■ ASSOCIATED CONTENT

Supporting Information

The Supporting Information is available free of charge at https://pubs.acs.org/doi/10.1021/acs.jpclett.2c00885.

Detailed description of the computational methods and models. Additional data on the electronic structure and Bader charges. All reaction pathways with initial, transition and final state structures considered in this work, as well as the binding of a H atom, as reactivity probe (PDF)

■ AUTHOR INFORMATION

Corresponding Author

Pablo G. Lustemberg − *Instituto de Catálisis y Petroleoquímica, CSIC, 28049 Madrid, Spain; Instituto de Fisica Rosario (IFIR), CONICET-UNR, 2000EZP Rosario, Santa Fe, Argentina;* orcid.org/0000-0003-4058-4023; Email: p.lustemberg@csic.es

Authors

Sanjaya D. Senanayake − *Chemistry Division, Brookhaven National Laboratory, Upton, New York 11973, United States;* orcid.org/0000-0003-3991-4232

José A. Rodriguez − *Chemistry Division, Brookhaven National Laboratory, Upton, New York 11973, United States;* orcid.org/0000-0002-5680-4214

M. Verónica Ganduglia-Pirovano − *Instituto de Catálisis y Petroleoquímica, CSIC, 28049 Madrid, Spain;* orcid.org/0000-0003-2408-8898

Complete contact information is available at: https://pubs.acs.org/10.1021/acs.jpclett.2c00885

Notes

The authors declare no competing financial interest.

The DFT data that support the findings of this study are available in Materials Cloud {https://www.materialscloud.org/home} with the identifier DOI: 10.24435/materialscloud:8y-7m. The data is also available from the authors upon reasonable request.

■ ACKNOWLEDGMENTS

This project received funding from the European Union's Horizon 2020 research and innovation programme under the Marie Skłodowska-Curie grant agreement No 832121. M.V.G.P. thanks the support by MICINN-Spain (RTI2018-101604−B-I00). Computer time provided by the RES (Red Española de Supercomputación) resources at the MareNostrum 4 (BSC, Barcelona), Altamira (IFCA, Cantabria) and La Palma (IAC, La Laguna, Tenerife) nodes is acknowledged. Computer time provided by the DECI resources at Finis Terrae II based in Spain at CESGA, with the support from PRACE aislb, is also acknowledged. This research was supported by the U.S. Department of Energy, Office of Science, Office of Basic Energy Sciences, under Award DE-SC0019360.

■ REFERENCES

(1) Thornton, P. K. Livestock production: recent trends, future prospects. *Philosophical transactions of the Royal Society of London. Series B, Biological sciences* **2010**, *365* (1554), 2853−2867.

(2) Tang, P.; Zhu, Q.; Wu, Z.; Ma, D. Methane activation: the past and future. *Energy Environ. Sci.* **2014**, *7* (8), 2580−2591.

(3) Bousquet, P.; Ciais, P.; Miller, J. B.; Dlugokencky, E. J.; Hauglustaine, D. A.; Prigent, C.; Van der Werf, G. R.; Peylin, P.; Brunke, E. G.; Carouge, C.; Langenfelds, R. L.; Lathière, J.; Papa, F.; Ramonet, M.; Schmidt, M.; Steele, L. P.; Tyler, S. C.; White, J. Contribution of anthropogenic and natural sources to atmospheric methane variability. *Nature* **2006**, *443* (7110), 439−443.

(4) Horn, R.; Schlögl, R. Methane Activation by Heterogeneous Catalysis. *Catal. Lett.* **2015**, *145* (1), 23−39.

(5) Schwarz, H.; Shaik, S.; Li, J. Electronic effects on room-temperature, gas-phase C−H bond activations by cluster oxides and metal carbides: The methane challenge. *J. Am. Chem. Soc.* **2017**, *139* (48), 17201−17212.

(6) Meng, X.; Cui, X.; Rajan, N. P.; Yu, L.; Deng, D.; Bao, X. Direct Methane Conversion under Mild Condition by Thermo-, Electro-, or Photocatalysis. *Chem.* **2019**, *5* (9), 2296−2325.

(7) Rodriguez, J. A.; Liu, P.; Wang, X.; Wen, W.; Hanson, J.; Hrbek, J.; Pérez, M.; Evans, J. Water-gas shift activity of Cu surfaces and Cu nanoparticles supported on metal oxides. *Catal. Today* **2009**, *143* (1−2), 45−50.

(8) Mohsenzadeh, A.; Richards, T.; Bolton, K. DFT study of the water gas shift reaction on Ni(111), Ni(100) and Ni(110) surfaces. *Surf. Sci.* **2016**, *644*, 53−63.

(9) Ebrahimi, P.; Kumar, A.; Khraisheh, M. A review of recent advances in water-gas shift catalysis for hydrogen production. *Emergent Mater.* **2020**, *3* (6), 881−917.

(10) Chen, W.-H.; Chen, C.-Y. Water gas shift reaction for hydrogen production and carbon dioxide capture: A review. *Appl. Energy* **2020**, *258*, 114078.

(11) Pal, D. B.; Chand, R.; Upadhyay, S. N.; Mishra, P. K. Performance of water gas shift reaction catalysts: A review. *Renew. Sust. Ener. Rev.* **2018**, *93*, 549−565.

(12) Salcedo, A.; Lustemberg, P. G.; Rui, N.; Palomino, R. P.; Liu, Z.; Nemsak, S.; Senanayake, S. D.; Rodriguez, J. A.; Ganduglia-Pirovano, M. V.; Irigoyen, B. Reaction pathway for coke-free methane steam reformingon a Ni/CeO_2 catalyst: Active sites and role of metal-support interactions. *ACS Catal.* **2021**, *11*, 8327−8337.

(13) Yang, W.; Wang, Z.; Tan, W.; Peng, R.; Wu, X.; Lu, Y. First principles study on methane reforming over Ni/TiO_2(110) surface in solid oxide fuel cells under dry and wet atmospheres. *Sci. China Mater.* **2020**, *63* (3), 364−374.

(14) Niu, J.; Wang, Y.; Qi, Y.; Dam, A. H.; Wang, H.; Zhu, Y.-A.; Holmen, A.; Ran, J.; Chen, D. New mechanism insights into methane

steam reforming on Pt/Ni from DFT and experimental kinetic study. *Fuel* **2020**, *266*, 117143.
(15) Lustemberg, P. G.; Palomino, R. M.; Gutierrez, R. A.; Grinter, D. C.; Vorokhta, M.; Liu, Z.; Ramirez, P. J.; Matolin, V.; Ganduglia-Pirovano, M. V.; Senanayake, S. D.; Rodriguez, J. A. Direct conversion of methane to methanol on Ni-Ceria surfaces: Metal-Support interactions and water-enabled catalytic conversion by site blocking. *J. Am. Chem. Soc.* **2018**, *140* (24), 7681−7687.
(16) Senanayake, S. D.; Rodriguez, J. A.; Weaver, J. F. Low temperature activation of methane on metal-oxides and complex interfaces: Insights from surface science. *Acc. Chem. Res.* **2020**, *53* (8), 1488−1497.
(17) Liu, Z.; Grinter, D. C.; Lustemberg, P. G.; Nguyen-Phan, T. D.; Zhou, Y.; Luo, S.; Waluyo, I.; Crumlin, E. J.; Stacchiola, D. J.; Zhou, J.; Carrasco, J.; Busnengo, H. F.; Ganduglia-Pirovano, M. V.; Senanayake, S. D.; Rodriguez, J. A. Dry reforming of methane on a highly-active Ni-CeO_2 catalyst: Effects of metal-support interactions on C-H bond Breaking. *Angew. Chem., Int. Ed. Engl.* **2016**, *55* (26), 7455−7459.
(18) Liu, Z.; Lustemberg, P.; Gutiérrez, R. A.; Carey, J. J.; Palomino, R. M.; Vorokhta, M.; Grinter, D. C.; Ramírez, P. J.; Matolín, V.; Nolan, M.; Ganduglia-Pirovano, M. V.; Senanayake, S. D.; Rodriguez, J. A. In situ investigation of methane dry reforming on Metal/Ceria(111) surfaces: Metal−Support interactions and C−H bond activation at low temperature. *Angew. Chem., Int. Ed.* **2017**, *56* (42), 13041−13046.
(19) Carrasco, J.; López-Durán, D.; Liu, Z.; Duchoň, T.; Evans, J.; Senanayake, S. D.; Crumlin, E. J.; Matolín, V.; Rodríguez, J. A.; Ganduglia-Pirovano, M. V. In situ and theoretical studies for the dissociation of water on an active Ni/CeO_2 catalyst: Importance of strong metal−support interactions for the cleavage of O−H bonds. *Angew. Chem., Int. Ed.* **2015**, *54* (13), 3917−3921.
(20) Lustemberg, P. G.; Ramírez, P. J.; Liu, Z.; Gutierrez, R. A.; Grinter, D. G.; Carrasco, J.; Senanayake, S. D.; Rodriguez, J. A.; Ganduglia-Pirovano, M. V. J. A. C. Room-temperature activation of methane and dry re-forming with CO_2 on Ni-CeO_2 (111) surfaces: Effect of Ce3+ sites and metal−support interactions on C−H bond cleavage. *ACS Catal.* **2016**, *6* (12), 8184−8191.
(21) Lustemberg, P. G.; Mao, Z.; Salcedo, A.; Irigoyen, B.; Ganduglia-Pirovano, M. V.; Campbell, C. T. Nature of the Active Sites on Ni/CeO_2 Catalysts for Methane Conversions. *ACS Catal.* **2021**, *11* (16), 10604−10613.
(22) Lustemberg, P. G.; Zhang, F.; Gutierrez, R. A.; Ramirez, P. J.; Senanayake, S. D.; Rodriguez, J. A.; Ganduglia-Pirovano, M. V. Breaking simple scaling relations through metal-support interactions: Room temperature activation of methane on Pt-CeO_2. *J. Phys. Chem. Lett.* **2020**, *11* (21), 9131−9137.
(23) Choudhary, T. V.; Goodman, D. W. Methane Activation on Ni and Ru Model Catalysts. *J. Mol. Catal. A-Chem.* **2000**, *163* (1), 9−18.
(24) Marsh, A. L.; Becraft, K. A.; Somorjai. Methane dissociative adsorption on the Pt(111) surface over the 300− 500 K temperature and 1−10 Torr pressure ranges. *J. Phys. Chem. B* **2005**, *109* (28), 13619−13622.
(25) Arcotumapathy, V.; Alenazey, F. S.; Al-Otaibi, R. L.; Vo, D.-V. N.; Alotaibi, F. M.; Adesina, A. A. Mechanistic investigation of methane steam reforming over Ce-promoted Ni/SBA-15 catalyst. *Appl. Petrochem. Res.* **2015**, *5* (4), 393−404.
(26) Jacobsen, C. J. H.; Dahl, S.; Clausen, B. S.; Bahn, S.; Logadottir, A.; Nørskov, J. K. Catalyst design by interpolation in the periodic table: Bimetallic ammonia synthesis catalysts. *J. Am. Chem. Soc.* **2001**, *123* (34), 8404−8405.
(27) Greeley, J.; Jaramillo, T. F.; Bonde, J.; Chorkendorff, I. B.; Norskov, J. K. Computational high-throughput screening of electrocatalytic materials for hydrogen evolution. *Nat. Mater.* **2006**, *5* (11), 909−13.
(28) Escudero-Escribano, M.; Malacrida, P.; Hansen, M. H.; Vej-Hansen, U. G.; Velázquez-Palenzuela, A.; Tripkovic, V.; Schiøtz, J.; Rossmeisl, J.; Stephens, I. E. L.; Chorkendorff, I. Tuning the activity of Pt alloy electrocatalysts by means of the lanthanide contraction. *Science* **2016**, *352* (6281), 73.
(29) De, S.; Zhang, J.; Luque, R.; Yan, N. Ni-based bimetallic heterogeneous catalysts for energy and environmental applications. *Energy Environ. Sci.* **2016**, *9* (11), 3314−3347.
(30) Studt, F.; Abild-Pedersen, F.; Bligaard, T.; Sørensen, R. Z.; Christensen, C. H.; Nørskov, J. K. Identification of non-precious metal alloy catalysts for selective hydrogenation of acetylene. *Science* **2008**, *320* (5881), 1320.
(31) Xiao, Z.; Hou, F.; Zhang, J.; Zheng, Q.; Xu, J.; Pan, L.; Wang, L.; Zou, J.; Zhang, X.; Li, G. Methane dry reforming by Ni-Cu nanoalloys anchored on periclase-phase MgAlOx nanosheets for enhanced syngas production. *ACS Appl. Mater. Interfaces* **2021**, *13*, 48838−48854.
(32) Sachtler, W. M. H.; Santen, v. R. A. Surface composition and selectivity of alloy catalysts. *Adv. Catal.* **1977**, *26*, 69−119.
(33) Carrasco, J.; Barrio, L.; Liu, P.; Rodriguez, J. A.; Ganduglia-Pirovano, M. V. Theoretical studies of the adsorption of CO and C on Ni(111) and Ni/CeO_2(111): Evidence of a strong metal−support interaction. *J. Phys. Chem. C* **2013**, *117* (16), 8241−8250.
(34) Mao, Z.; Lustemberg, P. G.; Rumptz, J. R.; Ganduglia-Pirovano, M. V.; Campbell, C. T. Ni nanoparticles on CeO_2(111): Energetics, electron transfer, and structure by Ni adsorption calorimetry, spectroscopies, and density functional theory. *ACS Catal.* **2020**, *10* (9), 5101−5114.
(35) Salcedo, A.; Irigoyen, B. DFT insights into structural effects of Ni−Cu/CeO_2 catalysts for CO selective reaction towards water−gas shift. *Phys. Chem. Chem. Phys.* **2021**, *23* (6), 3826−3836.
(36) Zhang, F.; Gutiérrez, R. A.; Lustemberg, P. G.; Liu, Z.; Rui, N.; Wu, T.; Ramírez, P. J.; Xu, W.; Idriss, H.; Ganduglia-Pirovano, M. V.; Senanayake, S. D.; Rodriguez, J. A. Metal−Support interactions and C1 chemistry: Transforming Pt-CeO_2 into a highly active and stable catalyst for the conversion of carbon dioxide and methane. *ACS Catal.* **2021**, *11* (3), 1613−1623.
(37) Latimer, A. A.; Aljama, H.; Kakekhani, A.; Yoo, J. S.; Kulkarni, A.; Tsai, C.; Garcia-Melchor, M.; Abild-Pedersen, F.; Norskov, J. K. Mechanistic insights into heterogeneous methane activation. *Phys. Chem. Chem. Phys.* **2017**, *19* (5), 3575−3581.
(38) An, W.; Zeng, X. C.; Turner, C. H. First-principles study of methane dehydrogenation on a bimetallic Cu/Ni(111) surface. *J. Chem. Phys.* **2009**, *131* (17), 174702.
(39) Chen, S.; Zaffran, J.; Yang, B. Descriptor design in the computational screening of Ni-based catalysts with balanced activity and stability for dry reforming of methane reaction. *ACS Catal.* **2020**, *10* (5), 3074−3083.
(40) Campbell, C. T. Bimetallic surface chemistry. *Annu. Rev. Phys. Chem.* **1990**, *41* (1), 775−837.
(41) Sachtler, W. M. H. The second Rideal lecture. What makes a catalyst selective? *Faraday Discuss. Chem. Soc.* **1981**, *72* (0), 7−31.
(42) Jiang, Z.; Fang, T. Dissociation mechanism of H_2O on clean and oxygen-covered Cu(111) surfaces: A theoretical study. *Vacuum* **2016**, *128*, 252−258.

https://doi.org/10.1021/acs.jpclett.2c00885
J. Phys. Chem. Lett. 2022, 13, 5589−5596